C.P. No. 720


MINISTRY OF AVIATION

*AERONAUTICAL RESEARCH COUNCIL*

*CURRENT PAPERS*

# Calculations of the Structure of Unsteady Rarefaction Waves in Oxygen/Argon Mixtures, Allowing for Vibrational Relaxation

*by*

*J. P. Appleton*

LONDON: HER MAJESTY'S STATIONERY OFFICE

1966

PRICE 6*s* 6*d* NET

U.D.C. No. 546.21 : 546.293 : 533.6.011.8

C.P. No.720

February 1963

# CALCULATIONS OF THE STRUCTURE OF UNSTEADY RAREFACTION WAVES IN OXYGEN/ARGON MIXTURES, ALLOWING FOR VIBRATIONAL RELAXATION

by

J. P. Appleton *

SUMMARY

Numerical computations have been performed to investigate the effect of molecular vibrational relaxation on the structure of one-dimensional unsteady rarefaction waves in oxygen and oxygen/argon mixtures. A more realistic relaxation equation than that used in the earlier work of Wood and Parker[1] has been incorporated in the calculations, and the results are presented in a manner permitting direct comparison with experiments.

A non-equilibrium flow feature illustrated by these results is that the vibrational temperature of gas which enters an ageing wave will at first decrease, closely following the translational temperature, until at some position within the wave it will depart rapidly from the translational temperature and eventually "freeze" at a constant value.

* *University of Southampton.* This work was carried out while the author was employed as a Vacation Consultant to the Ministry of Aviation at the Royal Aircraft Establishment, Farnborough.

Replaces R.A.E. Tech Note No. Aero 2873 - A.R.C. 24 933.

## LIST OF CONTENTS



## LIST OF ILLUSTRATIONS

## 1 INTRODUCTION

This theoretical investigation is primarily in support of an experimental programme which is being conducted at the Royal Aircraft Establishment, Farnborough, to study the molecular vibrational relaxation of oxygen in a one-dimensional unsteady rarefaction wave. Thus, the choice and the range of condition to be considered, together with the manner in which the theoretical results have been presented, were dictated by the experimental facility.

From the theoretical point of view, interest in the effect of an internally relaxing energy mode on the structure of a centred rarefaction wave stems from the work of Wood and Parker[1]. They carried out an analysis and numerical calculations, using a simple rate law to describe the vibrational relaxation, in order to clarify the role of the "frozen" and "equilibrium" speeds of sound in the propagation of expansion waves in relaxing gases. They demonstrated that, although the expansion wave propagates initially at the "frozen" sound speed, the portion of the wave which moves faster than the "equilibrium" sound speed of the undisturbed gas ahead of the wave is attenuated. As the wave ages its character approaches that of a wave which is propagating wholly at the equilibrium speed of sound. The results presented here confirm this conclusion.

The range of conditions covered here by the calculations for pure oxygen and an oxygen-argon mixture are those which can be conveniently produced in a shock tube behind incident shocks for which $M_s$ varies in the range 7·0 ~ 8·6, and $p_1$ is 10 mm Hg. The analysis makes use of a realistic rate equation in which the characteristic time for vibration, $\tau_v$, is provided by the Landau-Teller theory[2] which has been coupled with the experimental results of Camac[3] and Blackman[4]. (Wood and Parker simply assumed $\tau_v(p) \propto 1/p$.) The numerical constants which have been used in the expression for $\tau_v$ are those suggested by Camac; they appear to correlate the experimental data very well. Within the temperature range considered for pure oxygen, the energy in the molecular vibrational mode is approximately 15% of the static enthalpy. However, at the higher temperatures the gas is slightly dissociated and the dissociation energy amounts to about the same proportion of the static enthalpy as the vibrational energy. Fortunately, it may be shown that, under the conditions of interest, the characteristic time $\tau_R$ for chemical recombination is very much larger than $\tau_v$ and is greater than a typical transit time through the expansion wave by a sufficient factor for the recombination process to be assumed frozen.

The calculations were performed on a Ferranti "Mercury" digital computer at the Royal Aircraft Establishment using a finite difference procedure based on the method of characteristics. The results are presented for several stations, x, along the shock tube with the flow variables plotted against time.

The experimental programme makes extensive use of a double-beam sodium D-line reversal method of determining a temperature which is believed to follow molecular vibration, Gaydon et al[5a,b]. Thus, a temperature corresponding to the vibrational energy has been evaluated and presented as an auxiliary flow variable.

and for $O_2 \sim O_2$ collisions

$$C_i = 6{\cdot}0 \times 10^{-7} \text{ cm}^3 \text{ particle}^{-1} \text{ sec}^{-1} \quad .$$

The value of C in equation (6) is theoretically dependent on the type of collision process, but the best that can be done using Camac's[6] experimental results is to set it equal to the average value of $10{\cdot}4 \times 10^0$ °K. The characteristic vibrational temperature, $\theta_v$, for oxygen is 2228°K. The energy term, E(T), in equation (4) is the equilibrium vibrational energy evaluated at the local temperature

$$E(T) = R\,\theta_v\,n_{O_2}\left[\exp\left(\frac{\theta_v}{T}\right) - 1\right]^{-1} \quad . \tag{7}$$

Equations (1) to (4) together with the two state equations

$$p = \rho T R\,(n_A + n_{O_2}) \tag{8}$$

$$\imath = (C_{P_{O_2}}\,n_{O_2} + C_{P_A}\,n_A)\,T + E \tag{9}$$

complete a set of six equations in the unknowns p, ρ, T, ı, E and u, which are to be solved subject to the appropriate boundary conditions. The auxiliary equation which gives the vibrational temperature of the diatomic molecules is

$$T_v = \theta_v\left[\log_e\left(\frac{R\,\theta_v\,n_{O_2}}{E} + 1\right)\right]^{-1} \quad . \tag{10}$$

The theoretical flow model that is adopted is described by the wave diagram in the (x,t) plane of Fig.1. It is assumed that the right travelling incident shock heats the gas instantaneously to a uniform condition and that all the internal energy modes are immediately equilibrated with the translational mode. At the position x = t = 0, the shock sweeps away a weightless diaphragm, without reflection, which initially separates the test gas on its upstream side from a vacuum region on its downstream side. The result of this interaction is that a backward facing rarefaction (i.e. in Fig.1, a wave in which the gas enters from the left) propagates into the shocked test gas; the structure of this wave is the subject of the present investigation. Only in frozen or equilibrium flow would this wave be centred in the manner suggested in the figure.

## 3 THE METHOD OF SOLUTION

The system of equations (1) to (4) is hyperbolic and thus their solution will be sought using the method of characteristics. There are three characteristic curves in the (x,t) plane associated with the equations. By indicating

the directional derivatives along these curves with the subscripts (+), (-) and (o), the characteristic equations written

$$\left(\frac{dx}{dt}\right)_{\pm} = u \pm c \qquad (11), (12)$$

$$\left(\frac{dx}{dt}\right)_{o} = u \qquad (13)$$

$$\left(\frac{dp}{dt}\right)_{\pm} + \rho\, c \left(\frac{du}{dt}\right)_{\pm} + (\gamma - 1)\, \rho\, \frac{[E(T) - E]}{\tau_v} = 0 \qquad (14), (15)$$

$$\left(\frac{di}{dt}\right)_{o} = \frac{1}{\rho}\left(\frac{dp}{dt}\right)_{o} \qquad (16)$$

$$\left(\frac{dE}{dt}\right)_{o} = \frac{E(T) - E}{\tau_v} \qquad (17)$$

where

$$\gamma = \frac{C_{P_A} n_A + C_{P_{O_2}} n_{O_2}}{C_{P_A} n_A + C_{P_{O_2}} n_{O_2} - R(n_A + n_{O_2})} \qquad (18)$$

and the frozen sound speed, c, is given by

$$c^2 = \gamma R (n_A + n_{O_2}) T \ . \qquad (19)$$

## 3.1 The solution at $t \ll \tau_v$

Within this region of the rarefaction fan we see by dimensional arguments that E must remain essentially unchanged. In physical terms we are assuming the wave to be ideally centred and that although sufficient time has elapsed to allow enough collisions for equilibration of translation and rotation throughout the wave, no vibrational relaxation has occurred. The characteristic equations for this region are identical to those above with the omission of the terms containing $\tau_v$. Their solution is explicit and has been given extensively in the literature, for example by Courant and Freidrichs[7]. For the backward facing rarefaction under consideration here we have the (-) characteristics as a family of straight lines

$$\frac{x}{t} = u - c \qquad (20)$$

and

$$\frac{u}{2} + \frac{c}{\gamma - 1} = r_o \qquad (21)$$

where $r_o$ is a Riemann invariant, the value of which is given by evaluating the left hand side of equation (21) in the region ahead of the wave.

### 3.2 The solution at $t \gg \tau_v$

When t is very large the wave will have spread out, the gradients through it will have become small and the relatively large number of collisions necessary for the vibrational energy to approach equilibrium with the other energy modes will have had sufficient time to occur. Such reasoning leads us to put $E = E(T)$, but we see from equation (17) that this may only be true when $t \to \infty$. Therefore, we deduce that although the solution in the region $t \gg \tau_v$ may approach the equilibrium solution, it is never exactly equal to it. The equilibrium solution is obtained by replacing the rate equation (4) by equation (7) with E written instead of E(T). The characteristic equations are similar to those obtained for the frozen flow at t = 0 with the difference that c is replaced by a, the equilibrium speed of sound, which is given by the equation

$$a^2 = \gamma_e RT \left(n_A + n_{O_2}\right) \tag{22}$$

where

$$\gamma_e = \frac{C_{P_A} n_A + C_{P_{O_2}} n_{O_2} + \phi(T)}{C_{P_A} n_A + C_{P_{O_2}} n_{O_2} + \phi(T) - R\left(n_A + n_{O_2}\right)}$$

and

$$\phi(T) = \frac{1}{R\, n_{O_2}} \left(\frac{E}{T}\right)^2 \exp\left(\frac{\theta_v}{T}\right) .$$

The (-) characteristics are again a family of straight lines.

$$\frac{x}{t} = u - a \tag{23}$$

but this time the relationship between the velocity and the thermodynamic variables is obtained by numerically integrating the equation

$$\frac{dp}{du} = -\rho a . \tag{24}$$

### 3.3 The solution at intermediate values of t

The solutions at intermediate values of time have been obtained by a numerical method based on the characteristic grid in the (x,t) plane. First order difference equations which correspond to the characteristic relations (7) to (15) and a description of the general method of solution are given in Appendix (A). The calculation starts from the known initial conditions along the first straight (-) characteristic and the "frozen" flow solution which is known on each (-) characteristic at t = 0.

The integration interval size through the expansion at the origin was taken to be an incremental temperature. It was chosen by ensuring that the "frozen" flow solution obtained by numerically integrating the equation

$$\frac{dp}{du} = -\rho c \tag{25}$$

gave satisfactory agreement with the exact solution obtained from equation (21).

The integration interval in the direction away from the origin was given in terms of the time co-ordinate along the first (-) characteristic. The interval size was initially specified somewhat arbitrarily and then consistently varied until the subsequent solutions showed no significant variation with each other over a large portion of the flow field of likely interest. The final machine programme accepted a variable time interval along the first (-) characteristic as part of the input data. Having once established satisfactory interval sizes for one particular set of initial conditions, it was found that subsequent solutions were satisfactorily obtained for differing initial conditions by scaling the time intervals by a parameter, k. This parameter has the units of time and appears in the expression for the gradients of the flow variables through the wave head. The analysis for these wave head gradients is similar to that carried out by Wood and Parker. It determines the decay of the wave head due to the effects of relaxation; see Appendix (B). At the wave head

$$\left[\frac{\partial p}{\partial t} \Big/ \left(\frac{\partial p}{\partial t}\right)_f\right]_{x/t = u_2 - c_2} = \frac{kt \exp(-kt)}{1 - \exp(-kt)} \tag{26}$$

etc., where k is a function of the properties of the gas in region (2), and

$$(\Delta t.k)_i = (\Delta t.k)_s$$

where the subscript (i) refers to the flow conditions first considered and subscript (s) refers to subsequent initial conditions; $\Delta t$ is the incremental time interval along the first (-) characteristic.

The entire numerical procedure was programmed in autocode for use on a Ferranti "Mercury" computer.

## 4 DISCUSSION OF RESULTS

Oxygen was chosen as the test gas because it has a vibrational relaxation time short enough for the effects of relaxation on the structure of a rarefaction wave to be observable within typical shock tube running times e.g. $t \sim 10^{-4}$ secs, $M_s \sim 8$. Also, extensive temperature measurements have been made using the sodium D-line reversal method with oxygen in shock tubes.

The initial conditions chosen for the calculations were taken from the tables compiled by Bernstein[6] for incident shocks in oxygen. At the highest

shock Mach number considered the gas is 5% dissociated, however, the constant dissociation energy does not play any part in the calculations provided that no recombination takes place within the rarefaction. (A slight error is introduced by ignoring the contribution to the specific heat at constant pressure of the gas by the free atoms.) An expression defining a characteristic time for chemical recombination, $\tau_R$, is derived in Appendix (C) and the ratio, $\tau_v:\tau_R$, evaluated for the initial conditions considered here. Since $\tau_v \ll \tau_R$, it is unlikely that significant recombination could occur within the rarefactions during the experimental time scale.

The computed results are presented graphically in Figs.3 to 13. The flow variables have been plotted against time, measured from the instant the wave is formed, at several stations along the tube axis. Figs.3 to 10 represent the solution of a complete expansion for pure oxygen up to a distance of 12 inches from the diaphragm position. The initial temperature and pressure of the gas is 2478°K and 0·783 atmospheres respectively. Figs.11 to 13 illustrate the extent of results in the x-direction for three other sets of initial conditions. In these latter cases the expansions are not complete (i.e. the temperature and pressure are not reduced to zero) since experimental measurement of any flow property within the near vacuum end of the expansion would be most difficult. The initial conditions are given in Table 1 together with the appropriate incident shock Mach number for all the cases considered.

The results of main interest are those which show the variation of the vibrational temperature through the expansions. In the complete expansion, a fixed observer at any one of the downstream stations ($x_1$, $x_2$, etc., see Fig.1) will first see gas which has been expanded through the wave in its early history. During this rapid expansion the molecules will have suffered so few collisions that their vibrational energy will be unchanged. With increasing time the fixed observer will see gas which has been processed by the wave later in its history. The molecules will have had more opportunity to relax and a region will be observed in which the vibrational and translational temperatures are nearly equal. Fig.9 clearly illustrates that in this latter region, which is terminated by the passage of the wave head, both these temperatures lie very close to the translational temperature computed on the assumption of complete equilibrium. The proportion of the wave, within which close agreement between all three temperatures exists, increases with distance downstream. In the low pressure region at the tail end of the wave the translational temperature asymptotes to the appropriate "frozen" flow folution and the vibrational temperature returns to its initial value.

If these calculations had been performed in the Lagrangian frame of reference instead of in the (x,t) plane, it would have been easy to trace the history of a particular fluid element through the expansion fan. Then for such a fluid element which did not enter the wave until some time after its formation, the vibrational temperature would initially be in close agreement with the translational temperature but later depart rapidly from it and "freeze" at a constant value. Such behaviour is similar to that obtained in nozzle expansions of relaxing gases. This type of flow has received considerable attention starting with the initial numerical work due to Bray[8] who considered chemical non-equilibrium. More recently Blythe[9] has obtained an analytic solution for the distribution of molecular vibrational energy down a nozzle and has given an

expression for the final asymptotic "frozen" value of the vibrational energy; the restriction on his analysis is that the amount of energy in the lagging mode is very small.

The variation of the other flow properties through the rarefactions shows no unexpected behaviour. There is very little difference between the frozen and equilibrium pressure profiles through the wave and consequently a pressure transducer measurement at a downstream station would be the best way of relating optical temperature measurements to position within the rarefactions.

The effect of increasing either the initial temperature or density is to reduce $\tau_v$ which, in turn, increases the extent of near equilibrium flow within the wave at a given position from the diaphragm station. The reverse effect on the structure of the wave is achieved by diluting the oxygen with argon, since an argon atom is less efficient as a de-exciter than an oxygen molecule.

## 5 CONCLUDING REMARKS

Numerical solutions have been obtained, using a realistic vibrational relaxation equation for oxygen, which describe the structure of centred one-dimensional unsteady rarefaction waves. They have been presented in a form suitable for direct comparison with experiments.

The results show that the vibrational temperature of gas which enters an ageing wave will at first decrease, closely following the translational temperature, until at some position within the wave it will depart rapidly from the translational temperature and eventually "freeze" at a constant value. This behaviour is in keeping with the findings following theoretical investigations of non-equilibrium steady flow expansions.

Finally, the results confirm the conclusion due to Wood and Parker, namely, that the speed of propagation of an expansion wave in a relaxing gas will be initially that appropriate to "frozen" flow, but as the wave ages its character will change and approach that of a wave propagating under conditions of complete equilibrium.

## ACKNOWLEDGEMENTS

The author would particularly like to thank Mr. S. Popham for his assistance with the numerical computations and Dr. D.A. Spence for helpful discussions.

## LIST OF REFERENCES

| No. | Author(s) | Title, etc. |
|---|---|---|
| 1 | Wood, W.W.<br>Parker, F.R. | Structure of a centred rarefaction wave in a relaxing gas.<br>Physics of Fluids. 1, 3, 1958. |
| 2 | Landau, L.<br>Teller, E. | Zur theorie der schalldispersion.<br>Physik.Z. Savjetunion. 10, 34. 1936. |

## LIST OF REFERENCES (Contd.)


| No. | Author(s) | Title, etc. |
|---|---|---|
| 3 | Camac, M. | $O_2$ vibration relaxation in oxygen-argon mixtures. J.Chem. Physics. 34, 2, 1961. |
| 4 | Blackman, V.H. | Vibrational relaxation in oxygen and nitrogen. J. Fluid Mech. 1, 61, 1956. |
| 5(a) | Gaydon, A.G. | Energy transfer in hot gases. National Bureau of Standards. Circ.523, p.1. |
| 5(b) | Clouston, J.G.<br>Gaydon, A.G.<br>Hurle, I.R. | Temperature measurements of shock waves by spectrum line reversal. IIA double-beam method. Proc. Roy. Soc. A.252, pp.143-155, 1959. |
| 6 | Griffith, W.C. | Fundamental data obtained from shock tube experiments. Ed. A. Ferri. Pergamon Press, 1961. |
| 7 | Courant, R.<br>Friedrichs, K.O. | Supersonic flow and shock waves. Interscience Pub., Inc., N.Y. 1948. |
| 8 | Bray, K.N.C. | Atomic recombination in a hypersonic wind tunnel nozzle. J. Fluid Mech. 6, 1, 1959. |
| 9 | Blythe, P.A. | Non-equilibrium flow through a nozzle. N.P.L. Aero Rep. 1021, A.R.C.23, 871 June 1962. |
| 10 | Wray, K.L. | Chemical kinetics of high temperature air. Progress in Aeronautics and Rocketry, V.7. Ed. F.R. Riddel. Academic Press. 1961. |

## APPENDIX A

The first order difference equations corresponding to the characteristic equations (7) to (15) are

$$x_3 - x_1 = \tfrac{1}{2}(A_1 + A_3)(t_3 - t_1) \tag{1A}$$

$$x_3 - x_2 = \tfrac{1}{2}(B_2 + B_3)(t_3 - t_2) \tag{2A}$$

$$t_4 = \frac{(t_1 - t_2)}{(x_1 - x_2)} x_4 + \frac{(t_2 x_1 - t_1 x_2)}{(x_1 - x_2)} \tag{3A}$$

$$\frac{u_4 - u_2}{u_1 - u_2} = \frac{t_4 - t_2}{t_1 - t_2} \tag{4A}$$

$$x_3 - x_4 = \tfrac{1}{2}(u_3 + u_4)(t_3 - t_4) \tag{5A}$$

$$(p_3 - p_1) + \tfrac{1}{2}(D_1 + D_3)(u_3 - u_1) + \tfrac{1}{2}(F_1 + F_3)(t_3 - t_1) = 0 \tag{6A}$$

$$(p_3 - p_2) + \tfrac{1}{2}(D_2 + D_3)(u_2 - u_3) + \tfrac{1}{2}(F_2 + F_3)(t_3 - t_2) = 0 \tag{7A}$$

$$E_3 = E_4 + \tfrac{1}{2}(H_3 + H_4)(t_3 - t_4) \tag{8A}$$

$$i_3 = i_4 + \tfrac{1}{2}\left(\frac{1}{\rho_3} + \frac{1}{\rho_4}\right)(p_3 - p_4) \tag{9A}$$

where, $A = u + c$ $\qquad F = (\gamma - 1)\,\rho\,\dfrac{[E(T) - E]}{\tau_v}$

$B = u - c$

$D = \rho c$ $\qquad H = \dfrac{[E(T) - E]}{\tau_v}$

Consider the element of the characteristic grid, 1324, shown in Fig.2. We shall assume that the positions and the values of the flow variables at the points (1) and (2) are known from previous cycles of calculation and that everything at point (3) is to be calculated. A guess is first made for the flow variables and the coefficients $A_3$, $B_3$, etc., at point (3), then its co-ordinates, $(x_3, t_3)$ are obtained by solving the pair of simultaneous equations (1A) and (2A). The assumption that the flow variables have a linear variation along the straight line joining the points (1) and (2) is expressed by equations (3A) and (4A) which,

together with the difference equation (5A), may be solved to yield the co-ordinates of the point (4) on the particle path, (o), through (3). All the flow variables at the point (4) are then determined by interpolating between points (1) and (2). New values of $p_3$ and $u_3$ are obtained by solving the simultaneous equations (6A) and (7A) and the new values of $E_3$ and $i_3$ follow from (8A) and (9A) respectively. The coefficients $A_3$, $B_3$, etc. are recalculated and the whole sequence of operations is repeated until the difference between successive values of $T_3$, say, is sufficiently small. The calculations for the results presented here were performed to seven significant figures. The above general procedure was carried out in a step-by-step manner along each (- ) characteristic starting from the origin, $t = x = 0$.

## APPENDIX B

The analysis for the gradients of the flow variables through the wave head is best performed using the characteristic family parameters $\alpha$ and $\beta$ as the independent variables. The (—) family parameter is called $\alpha$ and is set equal to the slope of the (-) characteristic at the origin; the (+) family is called $\beta$ and is set equal to the value of t at which the (+) characteristic intersect the first (-) characteristic, $\alpha_1$, see Fig.2. The characteristic equations 7 to 15 may then be written in the form

$$\frac{\partial x}{\partial \alpha} = (u + c) \frac{\partial t}{\partial \alpha} \tag{1B}$$

$$\frac{\partial x}{\partial \beta} = (u - c) \frac{\partial t}{\partial \beta} \tag{2B}$$

$$\frac{\partial p}{\partial \alpha} + \rho c \frac{\partial u}{\partial \alpha} + (\gamma - 1) \rho \frac{[E(T) - E]}{\tau_v} \frac{\partial t}{\partial \alpha} = 0 \tag{3B}$$

$$\frac{\partial p}{\partial \beta} - \rho c \frac{\partial u}{\partial \beta} + (\gamma - 1) \rho \frac{[E(T) - E]}{\tau_v} \frac{\partial t}{\partial \beta} = 0 \tag{4B}$$

$$\frac{\partial E}{\partial \alpha} \frac{\partial t}{\partial \beta} + \frac{\partial E}{\partial \beta} \frac{\partial t}{\partial \alpha} = 2 \frac{[E(T) - E]}{\tau_v} \frac{\partial t}{\partial \alpha} \frac{\partial t}{\partial \beta} \tag{5B}$$

$$\frac{\partial i}{\partial \alpha} \frac{\partial t}{\partial \beta} + \frac{\partial i}{\partial \beta} \frac{\partial t}{\partial \alpha} = \frac{1}{\rho} \left( \frac{\partial p}{\partial \alpha} \frac{\partial t}{\partial \beta} + \frac{\partial p}{\partial \beta} \frac{\partial t}{\partial \alpha} \right) . \tag{6B}$$

Now along $\alpha_1$ we note that

$$\frac{\partial}{\partial \beta} [p(\alpha_1, \beta)] = 0 \text{ etc.}$$

$$\frac{\partial}{\partial \beta} [t(\alpha_1, \beta)] = 1$$

$$\frac{\partial}{\partial \beta} [x(\alpha_1, \beta)] = u_2 - c_2$$

and thus at the wave head equations (1B) to (6B) reduce to the following

$$x' = (u_2 + c_2)\, t' \tag{7B}$$

$$\frac{dx'}{d\beta} = (u_2 - c_2)\frac{dt'}{d\beta} + (u' - c') \tag{8B}$$

$$p' + \rho_2 c_2 u' = 0 \tag{9B}$$

$$\frac{dp'}{d\beta} - \rho_2 c_2 \frac{du'}{d\beta} + (\gamma - 1)\frac{\rho_2}{(\tau_v)_2}\,[E'(T) - E'] = 0 \tag{10B}$$

$$E' = 0 \tag{11B}$$

$$\imath' = \frac{p'}{p_2} \tag{12B}$$

where,

$$\left(\frac{\partial p}{\partial \alpha}\right)_{\alpha=\alpha_1} = p' \quad \text{etc.}$$

These equations together with the two equations of state and the equations for c and E(T) may be solved for all such derivatives as p', t', etc. Thus we obtain

$$p' = p'(o)\exp(-k\beta) \tag{13B}$$

and

$$t' = \frac{(\gamma + 1)^2}{4\,\rho_2 c_2}\,\frac{p'(o)}{k}\,[\exp(-k\beta) - 1] \tag{14B}$$

where

$$k = \frac{\gamma}{2}(\gamma - 1)^2\left(1 + \frac{n_A}{n_{o_2}}\right)\frac{E^2(T_2)}{c_2^4}\,\frac{1}{(\tau_v)_2}\exp\left(\frac{\theta_v}{T_2}\right). \tag{15B}$$

Now

$$\frac{\partial p}{\partial \beta} = \frac{\partial p}{\partial x}\frac{\partial x}{\partial \beta} + \frac{\partial p}{\partial t}\frac{\partial t}{\partial \beta}$$

$$\frac{\partial p}{\partial \alpha} = \frac{\partial p}{\partial x}\frac{\partial x}{\partial \alpha} + \frac{\partial p}{\partial t}\frac{\partial t}{\partial \alpha}$$

and thus at the wave head

$$p' = \left(\frac{\partial f}{\partial x}\right) x' + \left(\frac{\partial f}{\partial t}\right) t'$$

$$0 = \left(\frac{\partial f}{\partial x}\right) (u_2 - c_2)\, x' + \left(\frac{\partial f}{\partial t}\right) t'$$

therefore

$$\left(\frac{\partial p}{\partial t}\right)_{x/t=u_2-c_2} = - \frac{(u_2 - c_2)}{2\, c_2} \frac{p'}{t'} \quad . \tag{16B}$$

Substituting equations (13B) and (14B) into equation (16B) gives

$$\left[\frac{\partial p}{\partial t} \Big/ \left(\frac{\partial p}{\partial t}\right)_f\right]_{x/t=u_2-c_2} = \frac{kt \exp(-kt)}{1 - \exp(-kt)} \tag{17B}$$

where it may be shown from the "frozen" flow solution that

$$t\left[\left(\frac{\partial p}{\partial t}\right)_f\right]_{x/t=u_2-c_2} = \frac{2}{\gamma + 1} \rho_2 c_2 (u_2 - c_2) \, .$$

Expressions for the gradients of the other flow variables follow in a similar manner.

## APPENDIX C

A characteristic recombination time for weakly dissociated pure oxygen at constant density may be defined on the assumption that the dominant reaction is

$$O + O + O_2 \xrightarrow{k_b} O_2 + O_2$$

and then following the classical theory of physical chemistry we obtain the rate equation

$$W_o \frac{dn_o}{dt} = - k_b \rho^2 n_o^2$$

therefore

$$\frac{1}{W_o n_o} = k_b \frac{\rho^2}{W_o^2} t + \frac{1}{W_o N_o}$$

where $n_o = N_o$, when $t = 0$. The characteristic recombination time is defined as the time required for $n_o$ to fall to the value $N_o/2$,

therefore

$$\tau_R = \frac{W_o}{k_b \rho^2 N_o} .$$

The recombination rate coefficient, $k_b$, is taken from the summary of chemical kinetic data for air reported by Wray[10]

$$k_b = 1{\cdot}875 \times 10^9 T \left(\frac{118000}{RT}\right) \text{cm}^6 \text{ mole}^2 \text{ sec}^{-1} .$$

See Table 1 for numerical results.

## LIST OF SYMBOLS

| | |
|---|---|
| $Cp_i$ | specific heat of translation and rotation at constant pressure of $i^{th}$ species |
| E | molecular vibrational energy per unit mass |
| $M_s$ | incident shock Mach No. |
| R | universal gas constant |
| T | temperature |
| $W_i$ | molecular weight of $i^{th}$ species |
| a | equilibrium sound speed |
| c | frozen sound speed |
| i | enthalpy per unit mass |
| k | defined by equation (15B) |
| $n_i$ | mass concentration of $i^{th}$ specie (moles/gm of mixture) |
| p | pressure |
| t | time |
| u | velocity |
| x | space co-ordinate |
| $\alpha,\beta$ | characteristic family parameters |
| $\gamma$ | defined by equations (18) and (22) |
| $\rho$ | density |
| $\theta_v$ | characteristic vibrational temperature |
| $\tau$ | characteristic relaxation time |

All other symbols are defined in the text.

### Suffices

| | |
|---|---|
| A | argon atoms |
| O | oxygen atoms |
| $O_2$ | oxygen molecules |
| e | equilibrium |
| f | frozen - - - |
| 1 | conditions in front of incident shock ) |
| 2 | conditions behind incident shock ) See Fig.1 |

TABLE 1

| Case Nos. | $M_s$ | $\rho_2$ (atmos.) | $T_2$ (°K) | $W_o n_o$ | $\tau_R$ (sec × $10^6$) | $\tau_v$ (sec × $10^6$) | $\tau_R/\tau_v$ |
|---|---|---|---|---|---|---|---|
| 1 | 7·0 | 0·783 | 2478 | 0·008 | 3940 | 3·31 | 1190 |
| 4 | 7·6 | 0·915 | 2705 | 0·019 | 1493 | 1·61 | 928 |
| 3 | 8·6 | 1·21 | 2994 | 0·050 | 459 | 1·06 | 433 |

100% oxygen

| | | | | |
|---|---|---|---|---|
| 2 | 5·7 | 0·51 | 2478 | 50% oxygen, 50% argon by mass |

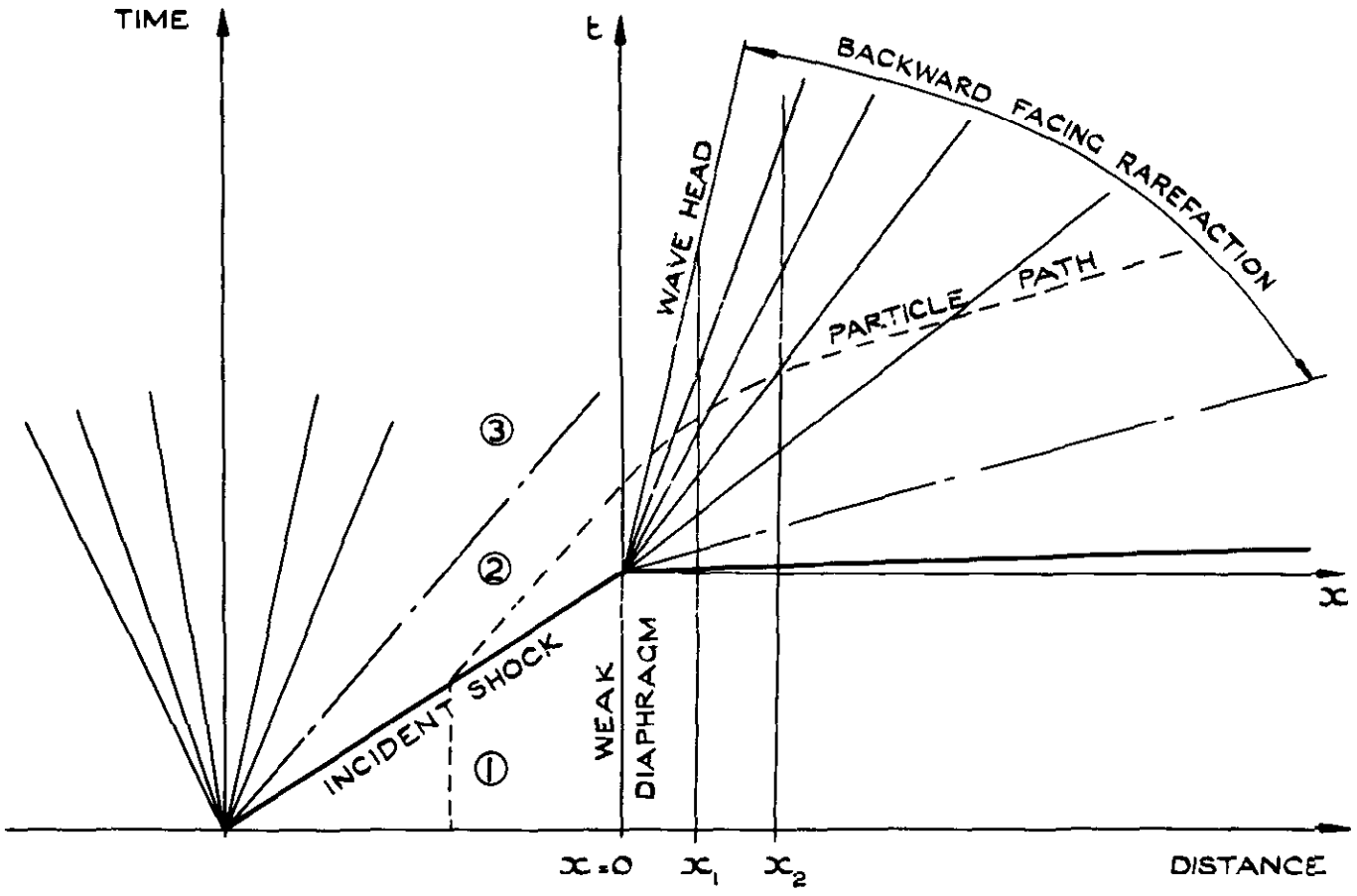


FIG. 1. FLOW GEOMETRY – SCHEMATIC.

(NOTE THAT ONLY IN FROZEN OR EQUILIBRIUM FLOW WOULD THE SECOND EXPANSION FAN BE CENTRED AS SHOWN)

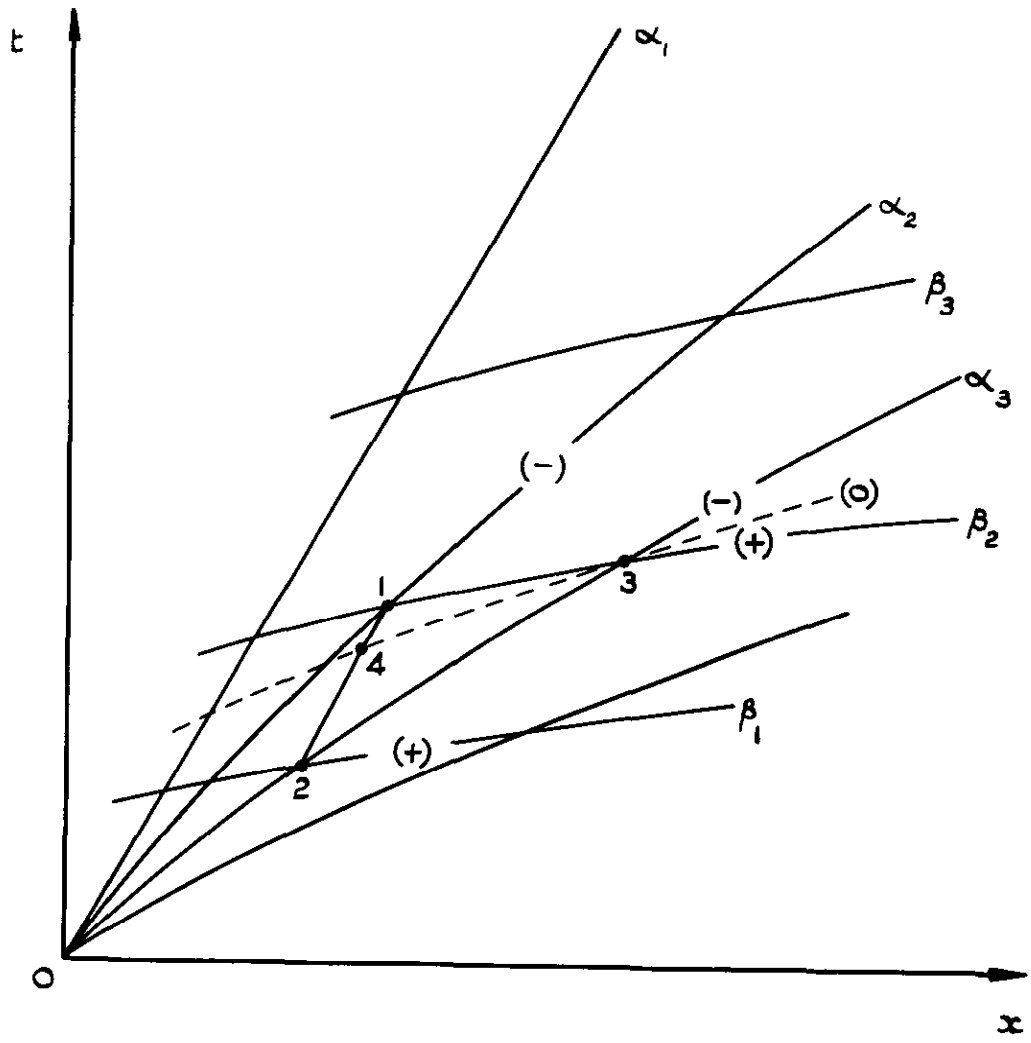


FIG. 2. CHARACTERISTIC GRID. (REFERRED TO IN APPENDIX A)

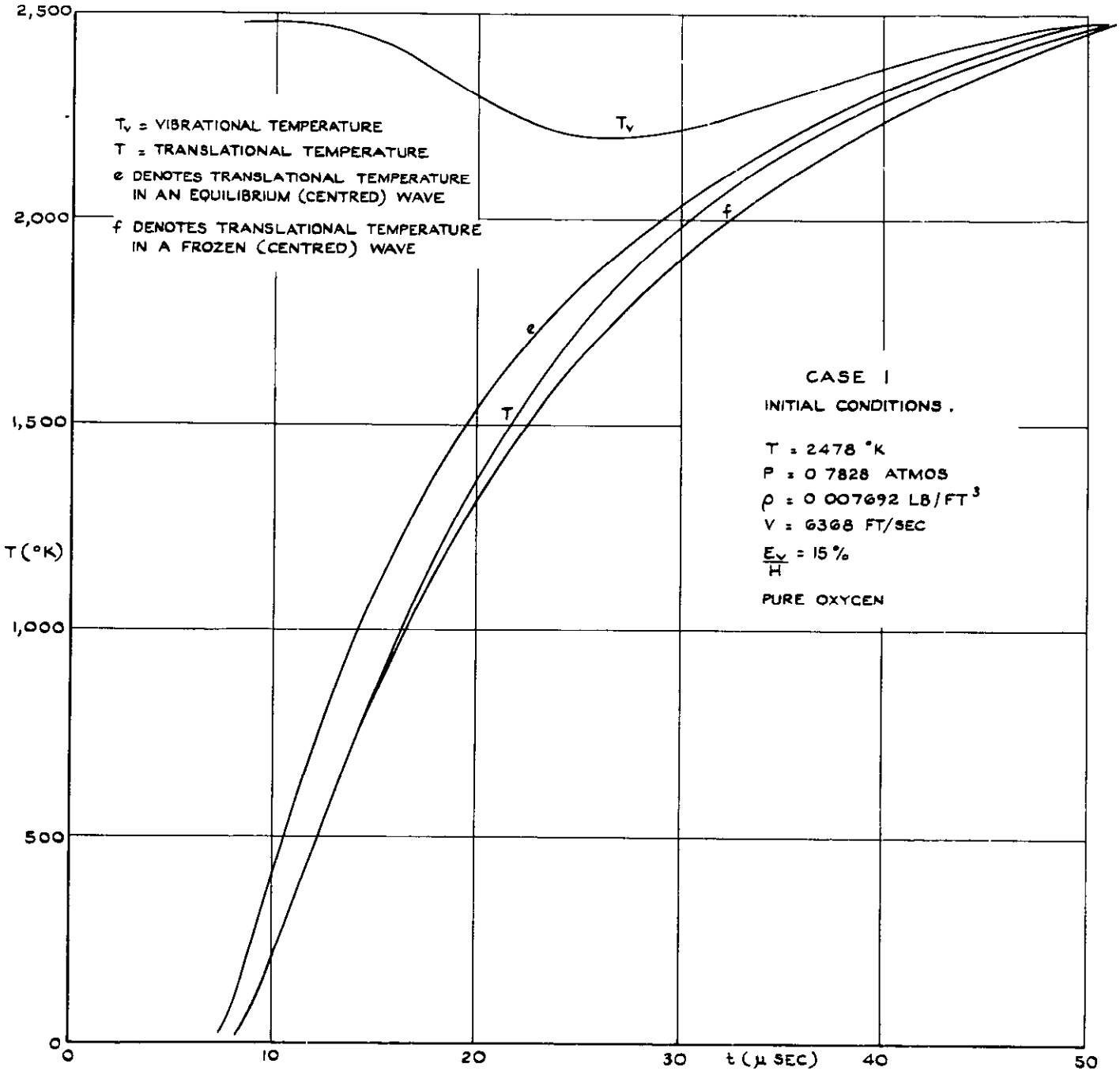


FIG 3 TEMPERATURE VARIATION IN EXPANSION WAVE IN PURE OXYGEN : CASE I, $T_2$ = 2478°K, x = 2 INCHES

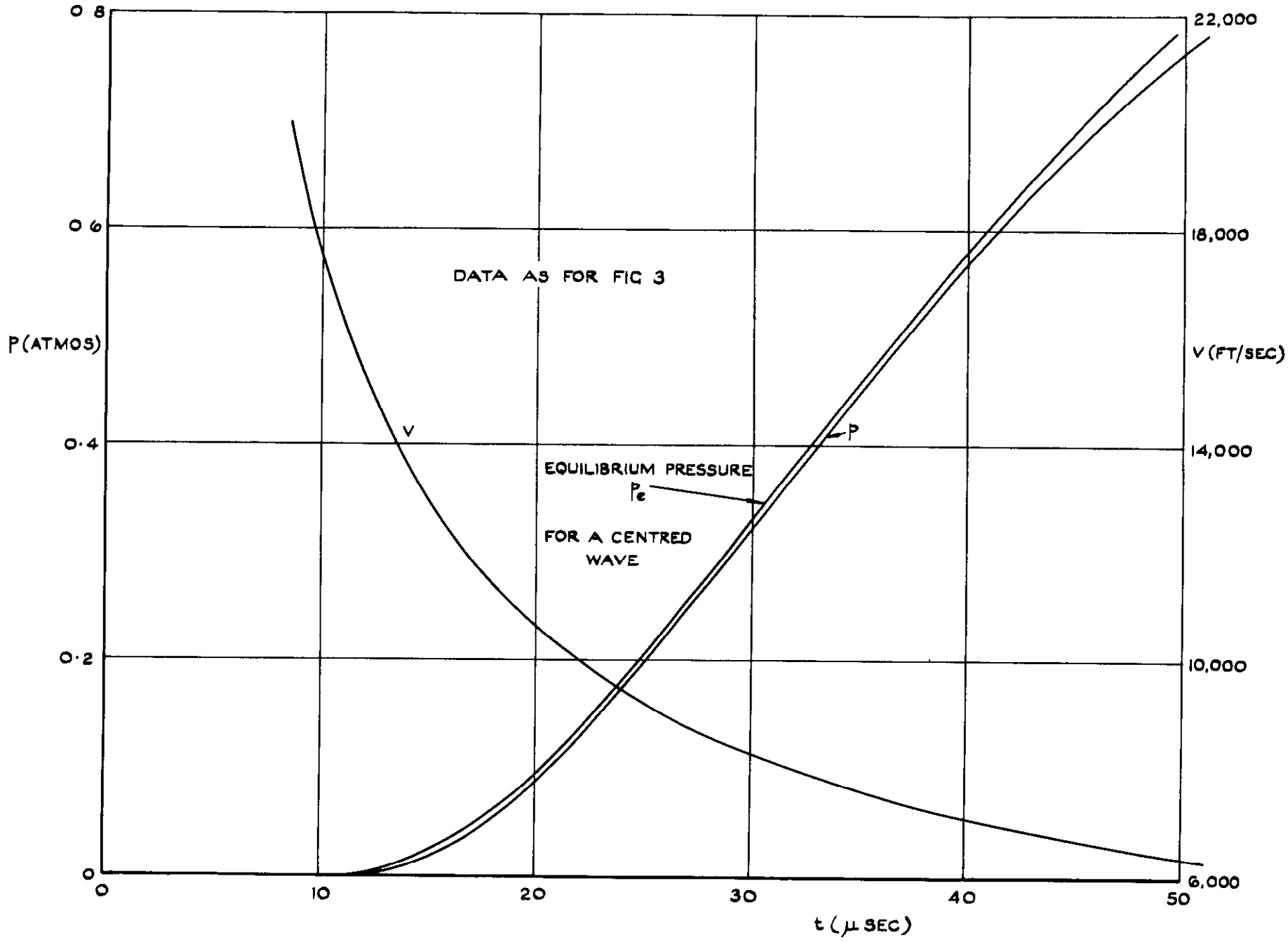


FIG. 4. PRESSURE AND VELOCITY IN EXPANSION WAVE : CASE 1, x = 2 INCHES.

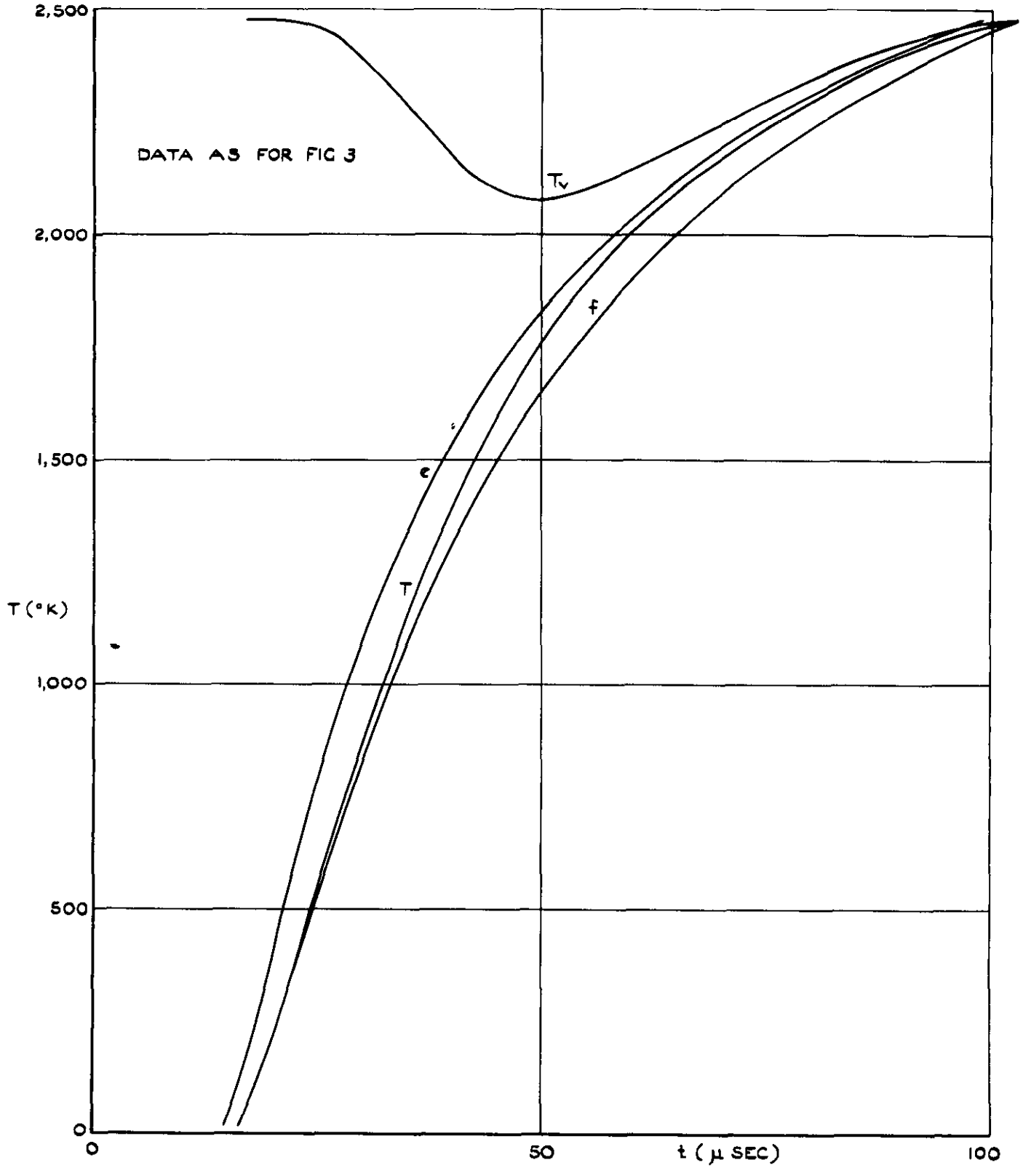


FIG. 5. TEMPERATURE VARIATION IN EXPANSION WAVE : CASE 1, x = 4 INCHES.

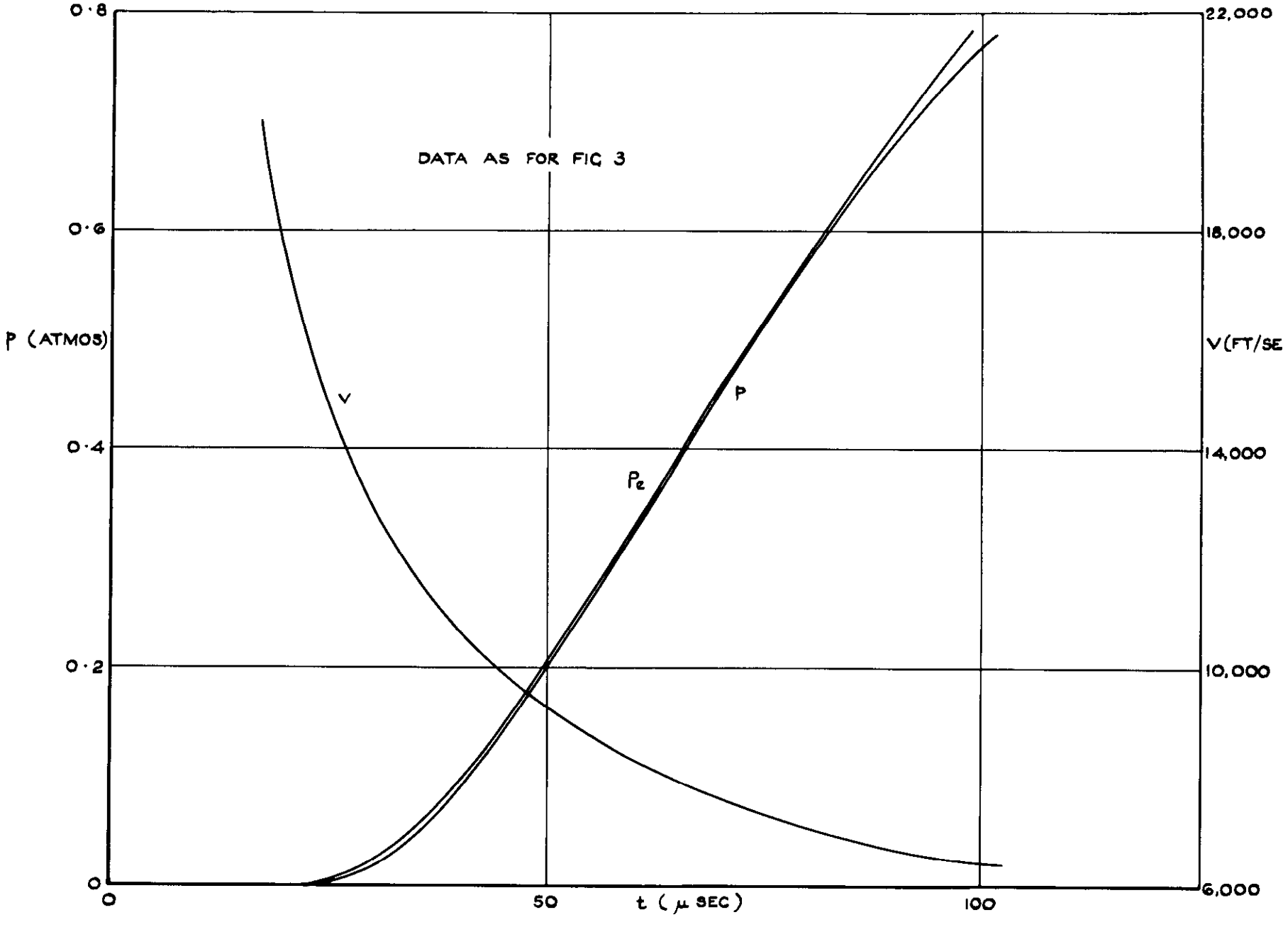


FIG. 6. PRESSURE & VELOCITY IN EXPANSION WAVE : CASE 1, x = 4 INCHES.

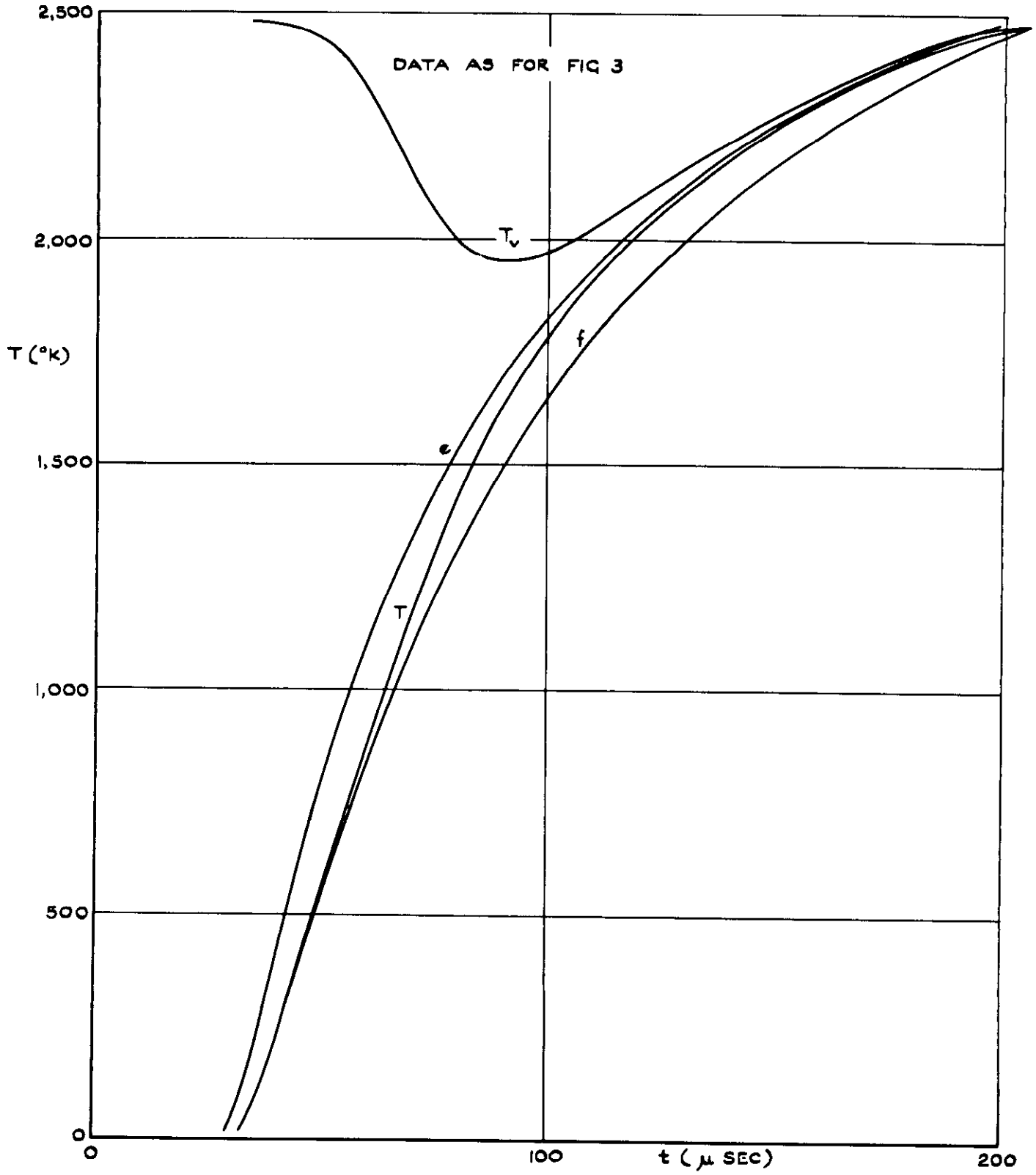


FIG. 7. TEMPERATURE VARIATION IN EXPANSION WAVE : CASE 1, x = 8 INCHES.

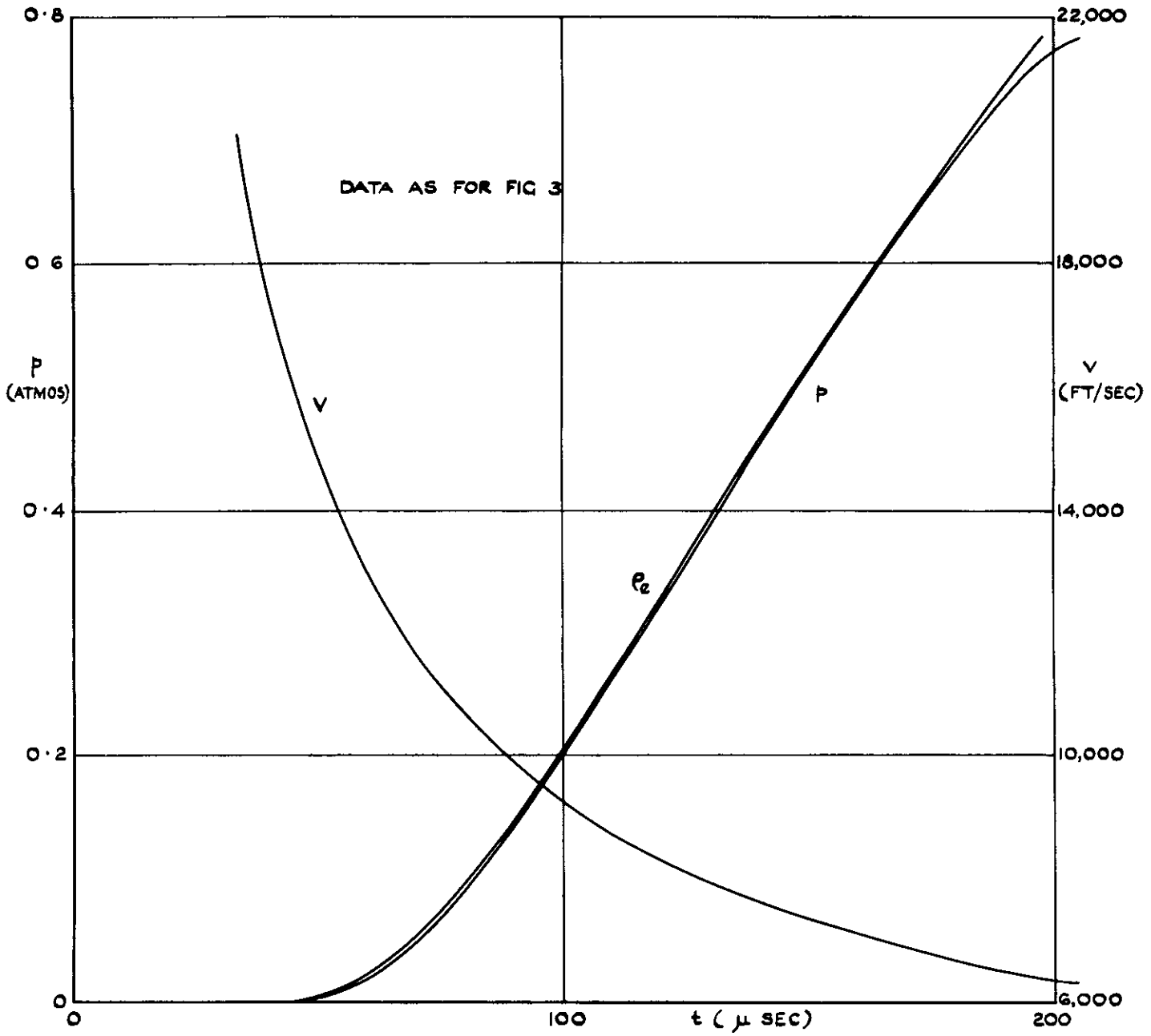


FIG. 8. PRESSURE & VELOCITY IN EXPANSION WAVE : CASE 1, x = 8 INCHES.

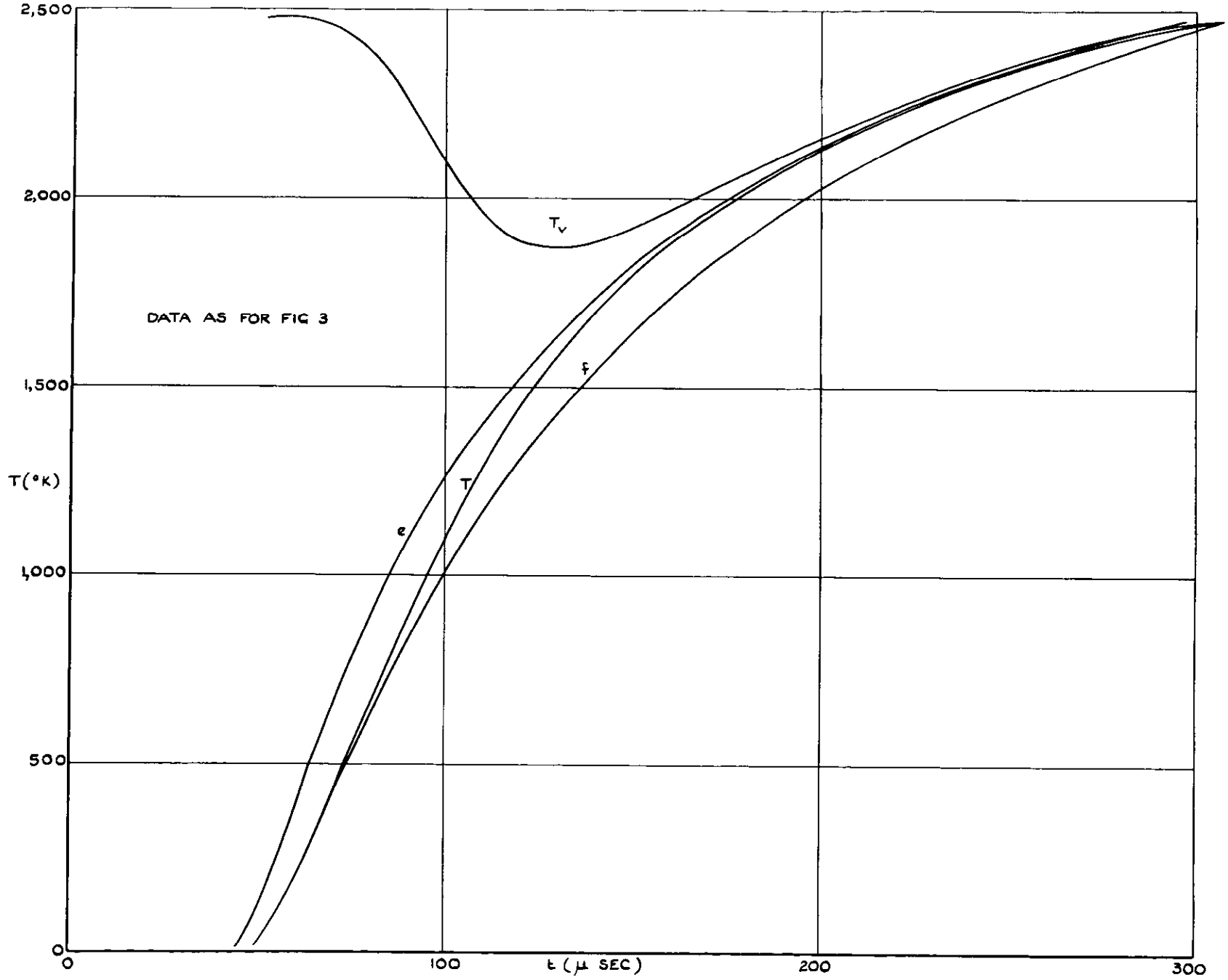


FIG 9 TEMPERATURE VARIATION IN EXPANSION WAVE : CASE 1, X = 12 INCHES

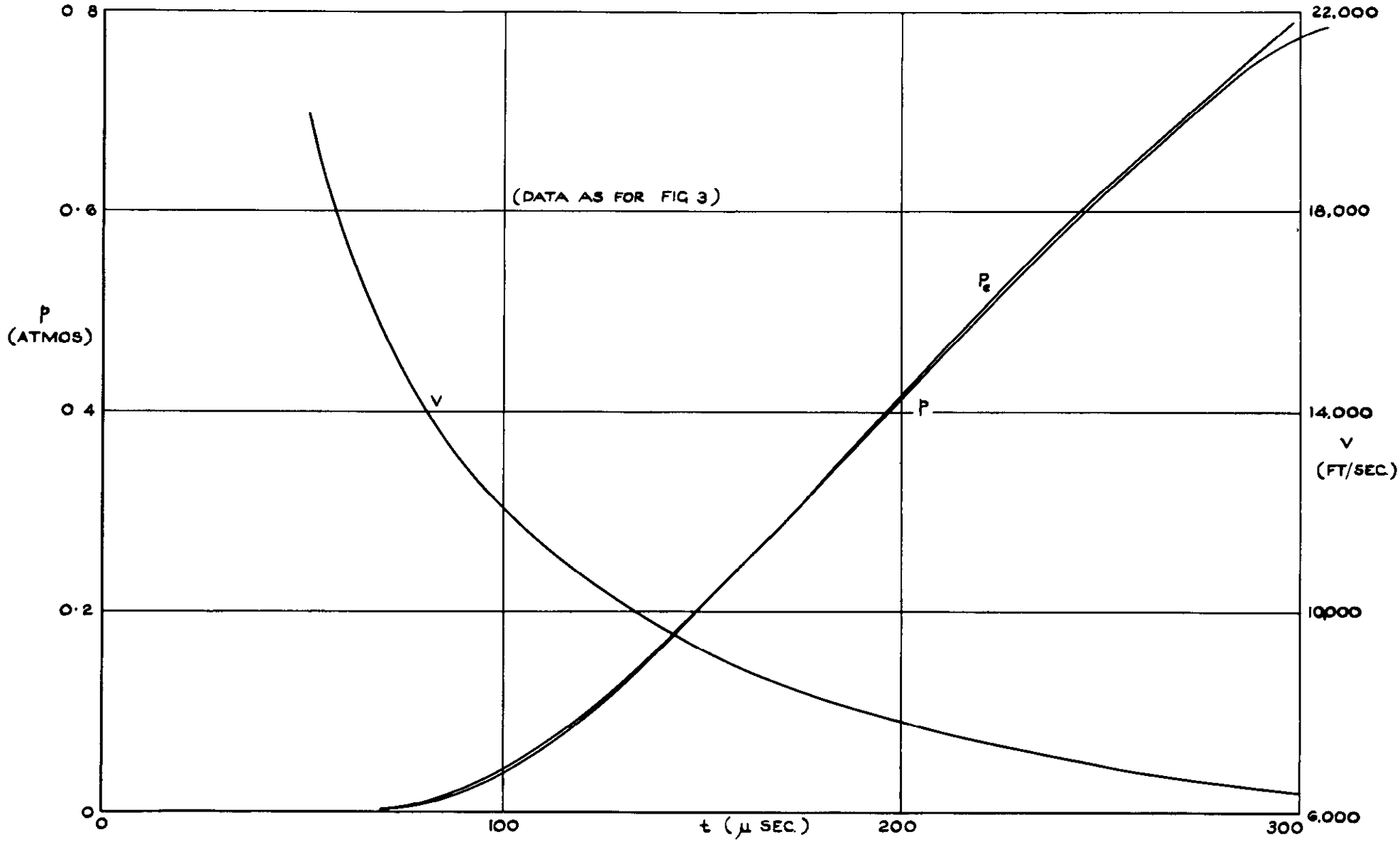


FIG. 10 PRESSURE & VELOCITY VARIATION IN EXPANSION WAVE:
CASE 1, X = 12 INCHES.

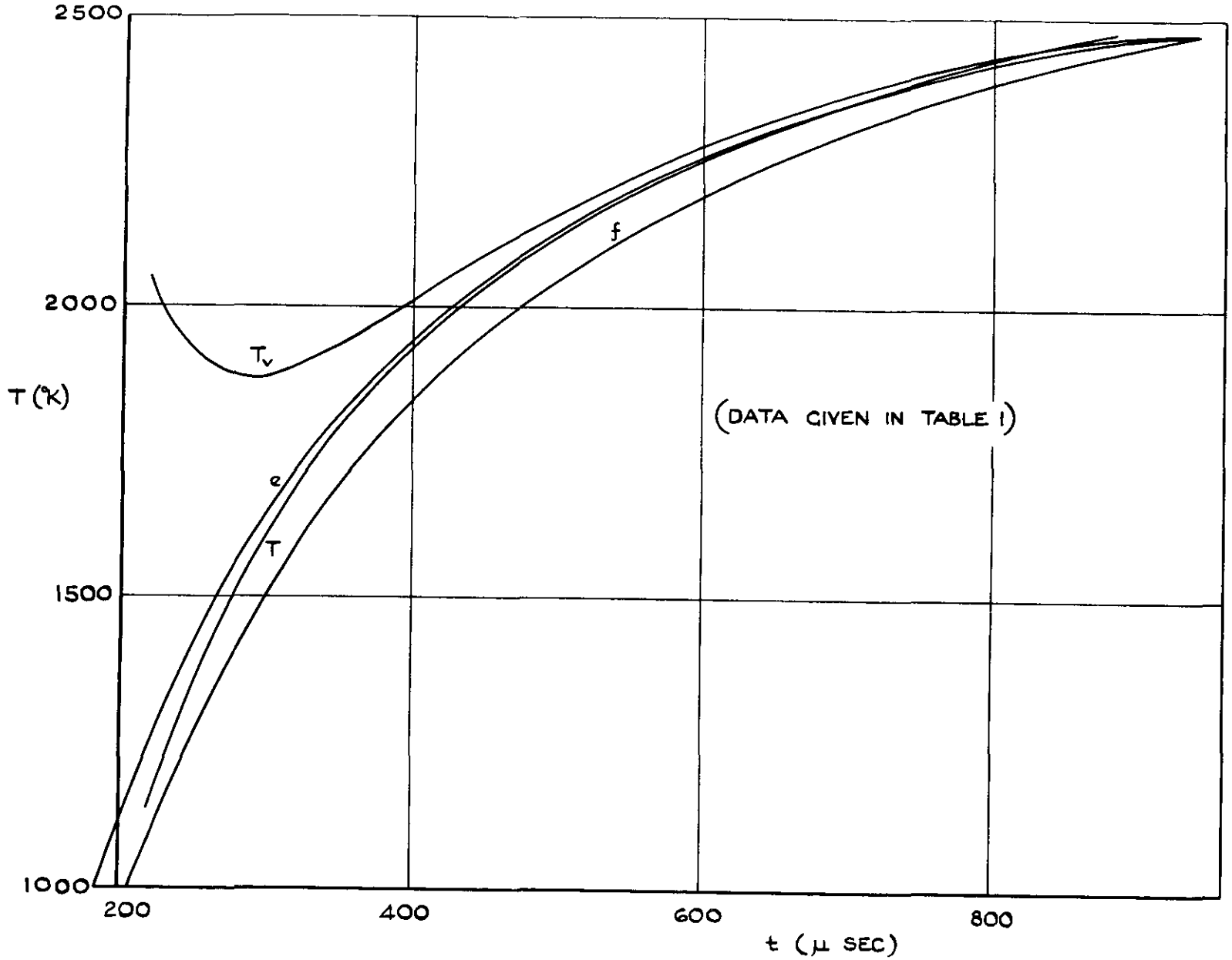


FIG. 11. TEMPERATURE VARIATION IN EXPANSION WAVE : CASE 2, 50% OXYGEN/ARGON MIXTURE. $T_2 = 2478°K$, X = 18 INCHES.

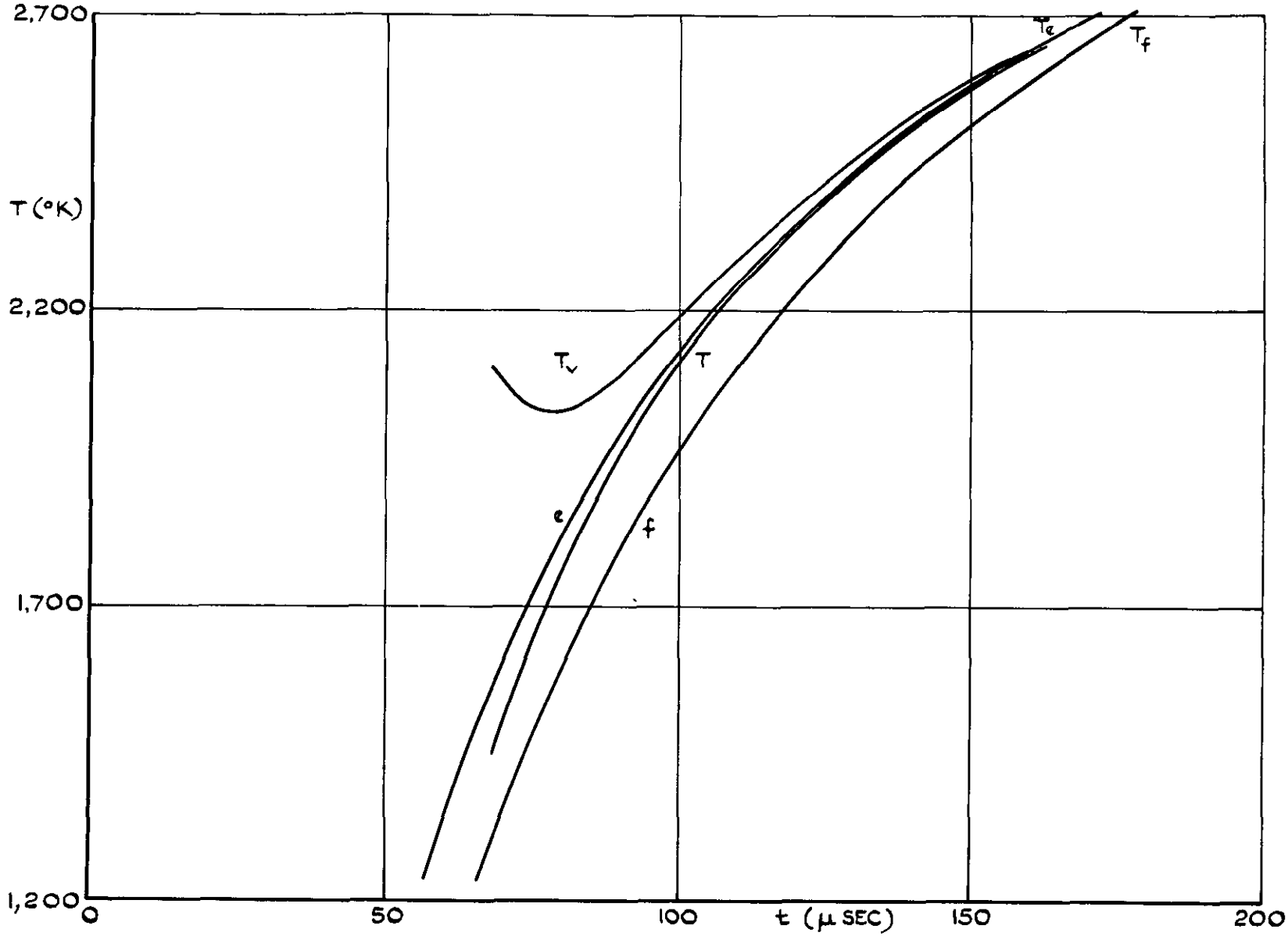


FIG. 12. TEMPERATURE VARIATION IN EXPANSION WAVE : CASE 4, PURE OXYGEN, $T_2 = 2705\,^{\circ}K$, x = 8 INCHES.

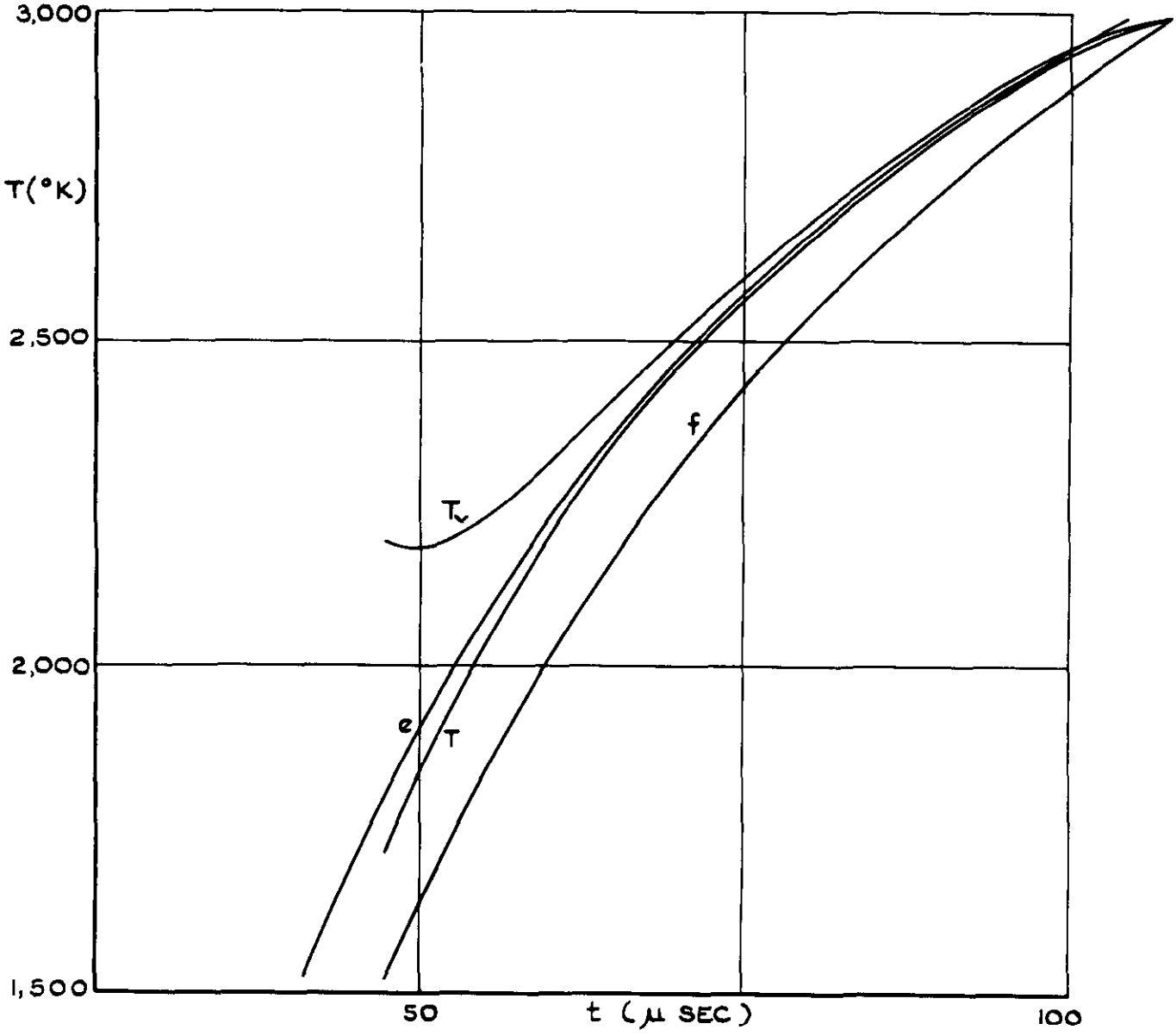


INITIAL CONDITIONS

$T$ = 2994 °K

$P$ = 1·2114 ATMOS

$\rho$ = 0·009853 P/Cu FT

$V$ = 8069 FT/SEC

$\frac{E_v}{H}$ = 0·16

$\gamma O_2$ = 1·0

$\gamma_A$ = 0

FIG13 TEMPERATURE VARIATION IN EXPANSION WAVE IN PURE OXYGEN: CASE 3, T = 2994°K, X = 6 INCHES.

*Printed in England for Her Majesty's Stationery Office by the Royal Aircraft Establishment, Farnborough. W T.59. K.4.*

A.R.C. C.P. No.720

546.21:
546.293:
533.6.011.8

CALCULATIONS OF THE STRUCTURE OF UNSTEADY RAREFACTION WAVES IN OXYGEN/ARGON MIXTURES, ALLOWING FOR VIBRATIONAL RELAXATION.
Appleton, J.P. February, 1963.

Numerical computations have been performed to investigate the effect of molecular vibrational relaxation on the structure of one-dimensional unsteady rarefaction waves in oxygen and oxygen/argon mixtures. A more realistic relaxation equation than that used in the earlier work of Wood and Parker[1] has been incorporated in the calculations, and the results are presented in a manner permitting direct comparison with experiments.

A non-equilibrium flow feature illustrated by these results is that the vibrational temperature of gas which enters an ageing wave will at

(Over)

A.R.C. C.P. No.720

546.21:
546.293:
533.6.011.8

CALCULATIONS OF THE STRUCTURE OF UNSTEADY RAREFACTION WAVES IN OXYGEN/ARGON MIXTURES, ALLOWING FOR VIBRATIONAL RELAXATION.
Appleton, J.P. February, 1963.

Numerical computations have been performed to investigate the effect of molecular vibrational relaxation on the structure of one-dimensional unsteady rarefaction waves in oxygen and oxygen/argon mixtures. A more realistic relaxation equation than that used in the earlier work of Wood and Parker[1] has been incorporated in the calculations, and the results are presented in a manner permitting direct comparison with experiments.

A non-equilibrium flow feature illustrated by these results is that the vibrational temperature of gas which enters an ageing wave will at

(Over)

A.R.C. C.P. No.720

546.21:
546.293:
533.6.011.8

CALCULATIONS OF THE STRUCTURE OF UNSTEADY RAREFACTION WAVES IN OXYGEN/ARGON MIXTURES, ALLOWING FOR VIBRATIONAL RELAXATION.
Appleton, J.P. February, 1963.

Numerical computations have been performed to investigate the effect of molecular vibrational relaxation on the structure of one-dimensional unsteady rarefaction waves in oxygen and oxygen/argon mixtures. A more realistic relaxation equation than that used in the earlier work of Wood and Parker[1] has been incorporated in the calculations, and the results are presented in a manner permitting direct comparison with experiments.

A non-equilibrium flow feature illustrated by these results is that the vibrational temperature of gas which enters an ageing wave will at

(Over)

DETACHABLE ABSTRACT CARDS

first decrease, closely following the translational temperature, until at some position within the wave it will depart rapidly from the translational temperature and eventually "freeze" at a constant value.

first decrease, closely following the translational temperature, until at some position within the wave it will depart rapidly from the translational temperature and eventually "freeze" at a constant value.

first decrease, closely following the translational temperature, until at some position within the wave it will depart rapidly from the translational temperature and eventually "freeze" at a constant value.

Published by
HER MAJESTY'S STATIONERY OFFICE
To be purchased from
49 High Holborn, London W C 1
423 Oxford Street, London W 1
13A Castle Street, Edinburgh 2
109 St Mary Street, Cardiff
Brazennose Street, Manchester 2
50 Fairfax Street, Bristol 1
35 Smallbrook, Ringway, Birmingham 5
80 Chichester Street, Belfast 1
or through any bookseller

C.P. No. 720

S.O. CODE No. 23-9015-20